Nuclear Inst, and Methods in Physics Research B 432 (2018) 13–19

Contents lists available at ScienceDirect

Nuclear Inst. and Methods in Physics Research B

journal homepage: www.elsevier.com/locate/nimb

# Localized transition models in luminescence: A reappraisal

George Kitis[a,*], Vasilis Pagonis[b]

[a] Aristotle University of Thessaloniki, Physics Department, Nuclear Physics and Elementary Particles Physics Section, 54124 Thessaloniki, Greece
[b] McDaniel College, Physics Department, Westminster, MD 21157, USA

ARTICLE INFO

*Keywords:*
Thermoluminescence
Localized transitions
Model
TL dosimetry
Stimulated luminescence
Lambert *W* function

ABSTRACT

Localized energy levels within the forbidden energy band are the source of various stimulated luminescence phenomena. The present study deals with the case of electrons stimulated from localized levels and recombining with a hole at a luminescence center, without the mediation of the conduction band. Previous research was based on three different assumptions as follows. Firstly, it was assumed that the recombination rate is independent of the concentration of recombination centers, and is proportional only to the concentration of electrons in the excited state of the trap. Secondly, it is assumed that the principle of detailed balance holds for these localized transitions. A third common assumption is that the system is in quasi-equilibrium condition. When these three conditions are applied to the system of differential equations describing the localized transitions, it was shown that the resultant thermoluminescence (TL) signals follow first order kinetics. This paper examines the assumptions used in these previous studies, and extensive simulations are carried out for a wide range of parameters in the localized transitions model. The results of the simulations show that the TL peaks in the localized model have very similar characteristics with TL peaks derived from delocalized models, including non-first order kinetic characteristics. The differential equations describing the localized transition model are solved analytically using the Lambert *W* function, and the resulting analytical master equation can describe a variety of optically and thermally stimulated phenomena.

## 1. Introduction

The models used to describe stimulated luminescence (SL) phenomena are phenomenological models based on the energy band theory of solids. Localized energy levels within the forbidden band are the source of several stimulated luminescence phenomena [1,2]. Three types of phenomenological models have been used extensively in the literature: delocalized models based on transitions involving the conduction and valence bands, localized models usually involving different energy levels of the traps/centers [1,3–5], and semilocalized models which are based on a combination of localized and delocalized energy levels [6,7]. For comprehensive historical summaries of these three types of luminescence models, the reader is referred to the relevant textbooks [1,2,8] and the recent review papers by Kumar et al. [9], Horowitz et al. [10], and Pagonis et al. [11].

There have been several types of localized models in the literature. In the original work by Halperin and Braner [3], during the thermal excitation stage electrons are raised into the excited state of the electron trap, from which they can either recombine at the recombination center, or they can be de-excited into the ground state. In this model, the conduction and valence bands participate in the kinetics only during the irradiation stage, and direct transitions from the conduction band into the ground or excited state of the trap are not allowed. Most importantly for the purposes of this paper, the rate of recombination in this model was assumed to depend on *both* the concentrations of electrons in the excited state of the trap, and on the concentration of holes in the center. Chen and Kirsh [1] suggested that each electron can only recombine with its closest neighbor in the crystal, and modified the differential equation of Halperin and Braner [3], so that the rate of recombination is proportional *only* to the concentration of electrons in the excited state. This assumption when combined with the assumption of a quasi- equilibrium state, leads to an analytical first order kinetics equation. Bull [4] used the same assumptions as Chen and Kirsh [1] and the same system of differential equations, to simulate characteristic TL glow curves in this localized model. The model parameters used by Bull [4] resulted in TL peaks with peak maximum temperatures ranging from 350 K to 2000 K. Bull [4] also noted some deviations from pure first order kinetics in their results, and reported symmetry factors as high as 0.48 for some parameters of their model.

A different type of localized tunneling recombination model has been proposed by Jain et al. [12], in which the distances between electron and hole traps are described by a specific spatial distribution.

* Corresponding author.
*E-mail address:* gkitis@auth.gr (G. Kitis).

https://doi.org/10.1016/j.nimb.2018.06.029
Received 6 June 2018; Received in revised form 28 June 2018; Accepted 28 June 2018

This model was solved analytically by Kitis and Pagonis [13], who obtained a master equation describing stimulated luminescence phenomena based on quantum tunneling. Using the resulting analytical equations these authors were able to analyze a great number of experimental data [14–17].

During the past decade there has been extensive experimental and simulation work on luminescence from nanodosimetric materials. Recent Monte Carlo simulations have shown that in materials with very high density of defects, the nearest neighbor approximation is not valid, and therefore each electron may interact with several of its neighbors (Pagonis and Truong [18]). In such cases of localized high densities of electrons and holes, one might expect that the original model by Halperin and Braner [3] would be a better approximation than the later model by Chen and Kirsh [1].

All previous modeling research on localized transitions has been based on the following three different assumptions:

(a) The recombination rate is independent of the concentration of recombination centers, and is proportional to the concentration for electrons in the excited state of the trap.
(b) The principle of detailed balance is assumed to hold for these localized transitions.
(c) The system is in quasi-equilibrium condition.

When these three conditions are applied to the system of differential equations describing the localized transitions, it was shown that the resultant thermoluminescence (TL) signals follow exclusively first order kinetics [8].

The aims of the present work are:

- To examine critically the assumptions used in these previous studies.
- To simulate the localized transition model using the original version of the model by Halperin and Braner [3], without the simplifications leading to first order kinetics.
- To examine if existing analytical expressions previously developed for delocalized models, can also describe luminescence signals simulated within localized transition models.
- To evaluate in detail the peak shape characteristics of the TL peaks, for a wide range of values of the parameters in the model.
- To derive new analytical expressions by solving the system of differential equations in the localized transition model, by following the method used by Kitis and Vlachos [26] for delocalized models, and by Kitis and Pagonis [13] for localized models.
- To investigate the role of the principle of detailed balance in the localized transition models.
- To investigate whether the localized transition model can describe additional stimulated luminescence phenomena, such as Linearly modulated optically stimulated luminescence (LM-OSL), continuous wave OSL (CW-OSL), isothermal TL (ITL).

## 2. The model

Lawless et al.[19] demonstrated that in order for a simulation to describe properly experimental results, it must contain all three stages of irradiation, relaxation and heating. The irradiation stage must always be followed by a relaxation stage, because carriers can build up to significant levels in the conduction and valence bands at the end of the irradiation stage. The relaxation stage provides the necessary time for the concentrations of charge carriers to decay to zero before the heating stage. Sadek and Kitis [20] showed that inclusion of the three stages is also a critical requirement for simulations. These authors examined critically the TL results of Kelly et al. [21] and Opanowitz [22], and found that most of the parameters used by these authors are not compatible with the irradiation stage, and therefore their pessimistic point view on the analysis of TL glow curves is not warranted.

It must be noticed, however, that one could in principle carry out the simulations in this paper by assuming equal initial concentrations of electrons and holes at the start of the heating stage; nevertheless, we have preferred to include all three stages for completeness.

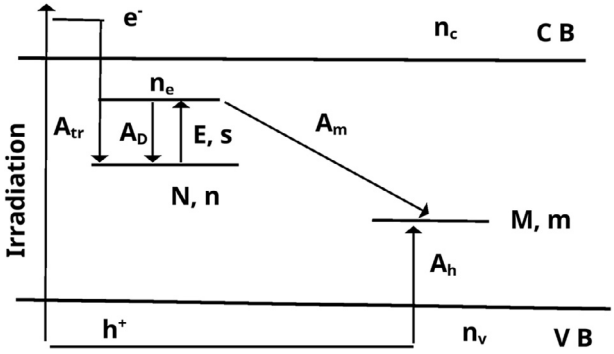


**Fig. 1.** Energy band diagram for the localized transition model.

In the present work we examine critically the original model of Halperin and Braner [3], by including the differential equations for the irradiation, relaxation and heating stages. More importantly, our study uses the original model without the later modifications by Chen and Kirsh [1] and Bull [4], which lead to first order kinetics.

The energy band diagram for the localized transition model is shown in Fig. 1. During irradiation electrons and holes are created in the conduction and valence bands, and are subsequently trapped into the ground state of the trap and the recombination center correspondingly. These transitions are indicated by $A_{tr}$ and $A_h$ in Fig. 1. During the heating stage electrons are raised into the excited state of electron trap, from which they can either recombine at the recombination center (transition $A_m$), or they can be de-excited into the ground state (transition $A_D$). As mentioned above, in this model the conduction and valence bands participate in the kinetics only during the irradiation stage.

The differential equations governing the traffic of free carriers during both the irradiation and heating stage are:

$$\frac{dT}{dt} = \beta, \tag{1}$$

$$\frac{dn}{dt} = -n\,p(t) + A_D\,n_e + A_{tr}(N-n)n_c, \tag{2}$$

$$\frac{dm}{dt} = A_h(M-m)n_v - A_m\,m\,n_e, \tag{3}$$

$$\frac{dn_e}{dt} = n\,p(t) - A_D\,n_e - A_m\,m\,n_e, \tag{4}$$

$$\frac{dn_v}{dt} = X - A_h(M-m)n_v, \tag{5}$$

$$\frac{dn_c}{dt} = X - A_{tr}(N-n)n_c. \tag{6}$$

The symbols on the diagram are: $N$ ($cm^{-3}$) is the concentration of available electron traps, $n$ ($cm^{-3}$) the concentration of trapped electrons, $M$ ($cm^{-3}$) is the concentration of available luminescence centers, $m$ ($cm^{-3}$) concentration of trapped holes. $n_c$ ($cm^{-3}$) and $n_v$ ($cm^{-3}$) are the concentration of electrons in the conduction and holes in the valence band. $A_{tr}$ ($cm^3\,s^{-1}$) is the trapping coefficient in electron traps and $A_h$ ($cm^3\,s^{-1}$) is the trapping coefficient of holes in luminescence centers. $E$ (eV) is the thermal activation energy, $s$ ($s^{-1}$) is the frequency factor and $k$ the Boltzmann constant, $\beta(K/s)$ is the heating rate and $X$ ($cm^{-3}\,s^{-1}$) is the rate of production of ion pairs per second and per $cm^{-3}$. This quantity is proportional to the dose rate. If the time of excitation is $t_e$, the total concentration of produced electron–hole pairs is $X{\cdot}t_e$ ($i.\,p.$ $cm^{-3}$), a quantity which is proportional to the total dose applied.

$n_e$ is the concentration of electrons in the excited state of the trap, $p(t)$ is the rate of excitation from the ground state energy level of the trap to the excited state, from which the electron can either recombine with a recombination coefficient $A_m$ ($cm^3\ s^{-1}$) or it can de-excite back into the ground state with a de-excitation coefficient $A_D$ ($s^{-1}$). The rate of excitation $p(t)$ depends on the type of experiment (LM-OSL, CW-OSL etc), and is of course different for thermal and optical excitation. For example, in TL experiments the rate of thermal excitation is $p(t) = s\,exp\left(-\frac{E}{kT}\right)$ , while in CW-OSL experiments the rate of optical excitation is constant $\lambda$ ($s^{-1}$), which depends on the optical cross section of the trap and on the intensity of the stimulating light source. In the case of LM-OSL experiments, the rate of excitation is varied linearly with time according to $p(t) = \lambda t/P$ , where $\lambda$ ($s^{-1}$) is the rate of optical excitation and $P$ is the total stimulation time during the LM-OSL experiment. The three stages are simulated with the above system of equations by using $\beta = 0$ for the irradiation stage, $\beta = 0$ and $X = 0$ for the relaxation stage, and $X = 0, A_{tr} = 0, A_h = 0$ for the heating stage.

An important point to note in these equations is that the recombination rate is written here in the form $-A_m\,m\,n_e$, in agreement with the original model of Halperin and Braner [3]. In the later versions of the model by Chen and Kirsh [1] and Bull [4], this term is written as $-\gamma\,n_e$, where $\gamma$ is a constant with dimensions of $s^{-1}$. In addition, the de-excitation term in the above equations is written here as $-A_D\,n_e$, while in these previous publications it is written as $-s\,n_e$ , based on the assumption that the principle of detailed balance is valid for the model (i.e. $A_D = s$).

According to the principle of detailed balance (PDB), the de-excitation rate coefficient $A_D$ must be equal to the frequency factor $s$. However, the PDB has been derived for a system in thermal equilibrium (Chen and Pagonis [8], Chapter 2), and experimental studies have raised the question whether it is applicable for systems in non-thermal equilibrium (Lloyd and Pake [23]). Furthermore, theoretical work has shown that the PDB principle applies only to cyclic systems (Klein [24], Thomsen [25]). As a consequence of these theoretical studies, the PDB will not be applicable in a multiple level model such as the localized model in Fig. 1.

In this paper we assume that the PDB does not apply, and study the consequences of this assumption on the model. Secondly, we use the original version of the model as written by Halperin and Braner [3], by writing the recombination rate in the form $-A_m\,m\,n_e$.

## 3. Analytical solution based on the Lambert *W* function

In this section the above system of differential equations is solved analytically, in order to obtain an expression for luminescence signals in the localized transition model.

Considering only the heating stage and assuming that the system is in quasi-equilibrium state [2], we set $dn_e/dt = 0$ in Eq. (4), to obtain the concentration of electrons in the excited state $n_e$:

$$n_e = \frac{n\,p(t)}{A_D + A_m\,m}. \tag{7}$$

By substituting this value of $n_e$ into Eq. (3):

$$\frac{dm}{dt} = -A_m\,m\,n_e = -p(t)\frac{n\,m\,A_m}{A_D + A_m\,m}. \tag{8}$$

and the luminescence intensity $I_{LOC}$ in the localized transition model will be:

$$I_{LOC} = -\frac{dm}{dt} = p(t)\frac{n\,m}{r + m},$$

where the ratio $r$ was defined as:

$$r = \frac{A_D}{A_m}. \tag{9}$$

We now make the common assumption that only a few electrons are in the excited state at any given moment, i.e. $n_e \ll n$ and therefore from the conservation of charge $m = n + n_e$ one obtains $m \approx n$. With this approximation,

$$I_{LOC} = -\frac{dn}{dt} = p(t)\frac{n^2}{r + n}, \tag{10}$$

Eq. (10) has the exact same mathematical form as the following general one trap (GOT) equation of the OTOR model (Kitis and Vlachos [26], their Eq. (11)):

$$I_{DEL} = p(t)\frac{n^2}{NR + n(1-R)}, \tag{11}$$

where the parameter $R$ in Eq. (11) is a dimensionless quantity, expressing the ratio of the retrapping and recombination coefficients $A_n$ and $A_m$ in the *delocalized* OTOR model:

$$R = \frac{A_n}{A_m}. \tag{12}$$

Kitis and Vlachos [26] showed that the solution of Eq. (11) for the *delocalized* OTOR model is given in terms of the Lambert $W(z)$ function (Corless et al. [27]):

$$I_{DEL} = p(t)\frac{RN}{(1-R)^2}\frac{1}{W[k, e^z] + W[k, e^z]^2} \tag{13}$$

$$z_{DEL} = \frac{RN}{n_0(1-R)} - ln\left[\frac{n_0\,|1-R|}{NR}\right] + \frac{1}{1-R}\int_{t_0}^{t} p(t)dt \tag{14}$$

where $k = 0$ or $k = -1$ for the two real branches of the $W(z)$ function, and $n_o$ is the initial concentration of trapped electrons.

From this point on, one follows closely the method of Kitis and Vlachos [26], and Eq. (10) can be integrated. After some extended but simple algebra, the following analytical solution is obtained for the *localized* model:

$$I_{LOC}(t) = p(t)\frac{r}{W[k, e^z] + W[k, e^z]^2} \tag{15}$$

$$z_{LOC} = \frac{r}{n_0} - ln\left[\frac{n_0}{r}\right] + \int_{t_0}^{t} p(t)dt \tag{16}$$

Eqs. (15) and (16) are master equations, similar to those obtained by Kitis and Vlachos [26] for the OTOR model, and by Kitis and Pagonis [13] for the localized tunneling recombination model of Jain et al. [12]. They are termed master equations because they provide a mathematical description for several types of stimulated luminescence phenomena, by selecting the appropriate expression for the excitation rate $p(t)$, as discussed above.

For TL and LM-OSL phenomena in the localized model, Eq. (16) for $z$ becomes correspondingly:

$$z_{LOC\text{-}TL} = \frac{r}{n_0} - ln\left[\frac{n_0}{r}\right] + s\int_{T_0}^{T} exp\left(-\frac{E}{k\,T}\right)dT \tag{17}$$

$$z_{LOC\text{-}LMOSL} = \frac{r}{n_0} - ln\left[\frac{n_0}{r}\right] + \frac{\lambda\,t^2}{2P} \tag{18}$$

It is important to note that the $r$ ratio in Eq. (9) is not a dimensionless quantity, but has units of $cm^{-3}$. By contrast, the parameter $R$ in Eq. (12) is a dimensionless quantity expressing the ratio of the retrapping and recombination coefficients in the *delocalized* OTOR model (Kitis and Vlachos [26]). It is also noted that Halperin and Braner [3] assumed that the principle of detailed balance holds, so that $r = s/A_m$ in their model. In the present paper, $r$ is used in the more general form of Eq. (9).

It is also necessary to note an important difference between the solutions of delocalized and localized models. In the case of delocalized model due to the presence of the term $(1-R)$ in denominator and of the logarithmic argument in Eq. (14), the solution is based on *both* real

branches of the Lambert $W$ function. On the other hand, in the case of localized model the solution in Eq. (15) is based *only* on the first real branch of the Lambert $W$ function, for any value of $r$.

By following the method of Kitis and Vlachos [26], one can now easily obtain the following condition for the temperature $T_m$ of maximum TL intensity:

$$\frac{\beta E}{k T_m^2} = F_{TL}\, s\, exp\left(-\frac{E}{k T_m}\right) \tag{19}$$

$$F_{TL} = \frac{1 + 2W[e^{z_m}]}{(1 + W[e^{z_m}])^2} \tag{20}$$

The corresponding condition for the time $t_m$ of maximum LM-OSL intensity is:

$$t_m^2 = F_{OSL}\, \frac{P}{\lambda} \tag{21}$$

$$F_{OSL} = \frac{(1 + W[e^{z_m}])^2}{1 + 2W[e^{z_m}]} \tag{22}$$

In both of these expressions, $z_m$ is the value of $z$ at $T = T_m$ and $t = t_m$, for TL and LM-OSL correspondingly.

## 4. Simulation results

### 4.1. The range of parameters used in the simulations

As discussed above, this paper presents a more general form of the localized model, in which the PDB principle does not apply, i.e. the condition $A_D = s$ is not valid. The values of $A_D$ in the simulations were then varied starting from a low value of $A_D = 10^{-2}$ s$^{-1}$ and increasing towards the value of $A_D = s$, which is predicted by the PDB.

The fixed parameter values used in the model were: $N = 10^{10}$ cm$^{-3}$, $M = 1.01 \times 10^{10}$ cm$^{-3}$, $A_h = A_{tr} = 10^{-7}$ cm$^3$ s$^{-1}$, thermal activation energy $E = 1$ eV, frequency factor $s = 10^{13}$ s$^{-1}$, dose rate $X = 10^7$ (cm$^{-3}$ s$^{-1}$).

The following detailed protocol was followed in the simulations:

- For given values of $A_m$, the $A_D$ values were varied in the range $10^{-2}$–$10^7$ s$^{-1}$ i.e. they cover 9 orders of magnitude. This $A_D$ sequence was simulated for 4 different values of $A_m$ : $10^{-8}$, $10^{-7}$, $10^{-6}$ and $10^{-5}$ cm$^3$ s$^{-1}$.
- For a given value of $A_D$, the dose was varied from $10^6$ to $10^{10}$ (cm$^{-3}$). The dose sequence was simulated for $A_D$ values in the range $10^{-2}$–$10^7$ s$^{-1}$. In these simulations the value $A_m = 10^{-7}$ cm$^3$ s$^{-1}$ was kept constant.

### 4.2. Simulation as function of de-excitation probability ($A_D$)

An important question about the localized model in this paper, is whether the model can produce non-first order kinetics. The answer is not obvious, since the values of the parameters are such that the PDB is not applicable in our simulations. To answer this question, the values of the de-excitation constant $A_D$ are varied first, while the value of $A_m$ is kept constant. Then the simulations are repeated for various $A_m$ values.

The primary purpose of these simulations was to see the effect of the PDB not being fulfilled in the localized model. A second goal of these simulations was to see how the temperature of maximum TL intensity $T_m$ and the symmetry factor $\mu_g$ of the simulated peaks behave as a function of the dose. A third goal was to investigate whether non-first order kinetics is possible within the model.

Fig. 2 shows characteristic TL peaks obtained by keeping the value $A_m = 10^{-7}$ cm$^3$ s$^{-1}$ constant, and varying the value of $A_D$ to obtain peaks (1): $10^{-1}$ s$^{-1}$, (2): $10^0$ s$^{-1}$, (3): $10^3$ s$^{-1}$, (4): $10^4$ s$^{-1}$ , (5): $10^4$ s$^{-1}$, (6): $10^6$ s$^{-1}$ and (7): $10^{13}$ s$^{-1}$. All peaks derived with $A_D$ from $10^{-2}$ s$^{-1}$ up to $10^0$ s$^{-1}$ were identical with TL peak labeled (1) in Fig. 2. Their symmetry factor

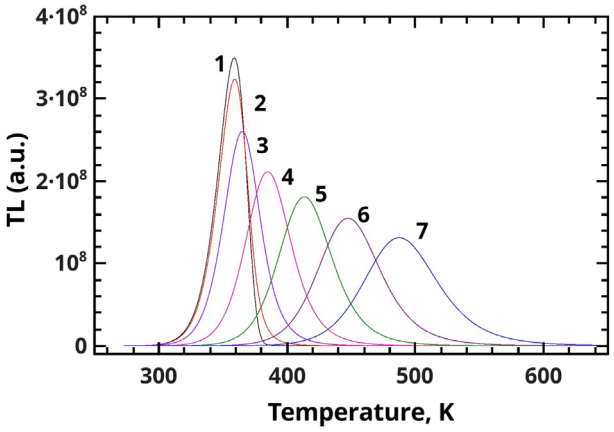


**Fig. 2.** Glow peak shape simulated using $A_m = 10^{-7}$ cm$^3$ s$^{-1}$ and a variable $A_D$ (s$^{-1}$) (1): $10^{-1}$, (2): $10^2$, (3): , (4): $10^4$, (5): $10^5$, (6): $10^6$, (7): $10^7$.

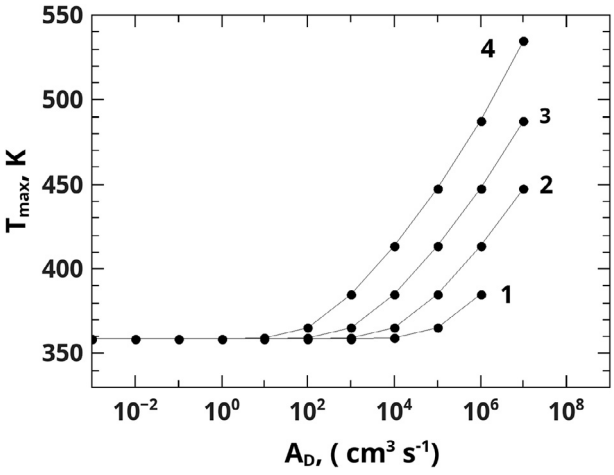


**Fig. 3.** Peak maximum temperature as a function of $A_D$ using a variable $A_m$ (cm$^3$ s$^{-1}$) (1): $10^{-5}$, (2): $10^{-6}$, (3): $10^{-7}$, (4): $10^{-8}$.

was $\mu_g = 0.42$, which corresponds to first order kinetics. As the value of $A_D$ exceeds $10^0$ s$^{-1}$ and increases towards $10^{13}$ s$^{-1}$, the peak maximum temperature starts to shift to higher temperatures, with a simultaneous broadening of the peak. Borrowing a term from the delocalized OTOR model, this is a clear indication of the increase of the kinetic order.

Fig. 3 shows the behavior of $T_m$ as a function of $A_D$. For values of $A_D$ up to $10^1$ s$^{-1}$, there is no shift of the value of $T_m$ , which is characteristic of first order kinetics. As $A_D$ exceeds the value of $10^1$ s$^{-1}$, a shift of $T_m$ towards higher temperatures emerges. Furthermore, this shift in $T_m$ depends also on the value of recombination probability $A_m$. The curves in Fig. 3 corresponds to $A_m$ values of (1): $10^{-5}$ cm$^3$ s$^{-1}$ (2): $10^{-6}$ cm$^3$ s$^{-1}$, (3): $10^{-7}$ cm$^3$ s$^{-1}$ and (4): $10^{-8}$ cm$^3$ s$^{-1}$.

A good measure of the kinetic order is the symmetry factor $\mu_g$ of the peak [3,28–31]. The value of $\mu_g$ is evaluated and its values as a function of $A_D$ are shown in Fig. 4. The obvious conclusion is that for all $A_D$ values up to $10^0$ s$^{-1}$ the resulting TL peaks have $\mu_g = 0.42$, which corresponds to first order kinetics. For higher values of $A_D$ one sees a trend towards second order kinetics and a value of $\mu_g = 0.52$, depending upon the values of $A_m$. This is the exact same behavior shown in the simulations of Fig. 3.

### 4.3. Simulation as function of dose

The second series of simulations investigates the behavior of TL peaks as a function of dose, which is one of the main characteristics of a dosimetric material. The goal here is to examine how $T_m$ varies as a

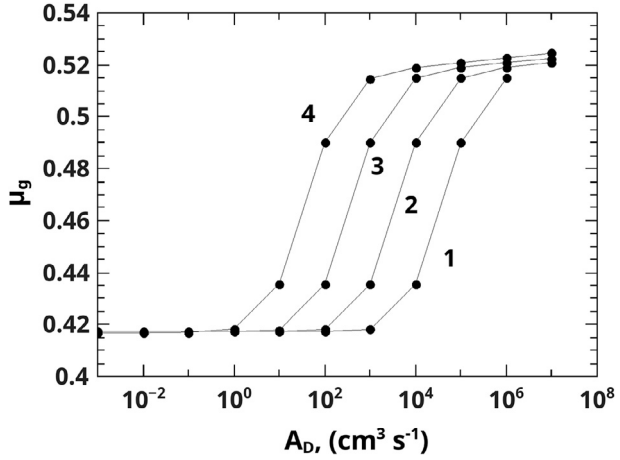


**Fig. 4.** Symmetry factor as a function of $A_D$, using a variable $A_m$ ($cm^3\,s^{-1}$) (1): $10^{-5}$, (2): $10^{-6}$, (3): $10^{-7}$, (4): $10^{-8}$.

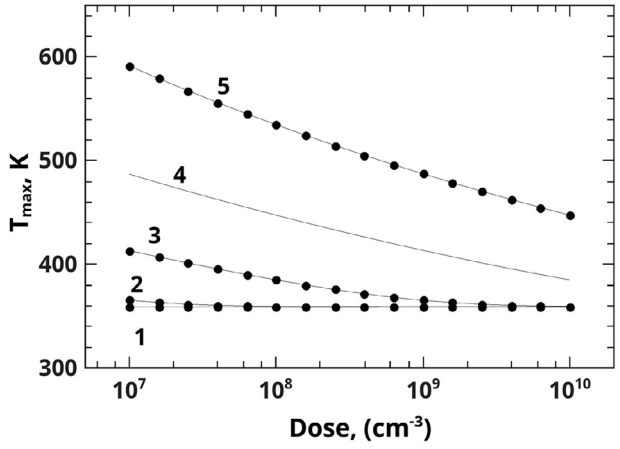


**Fig. 5.** Peak maximum temperature as a function of dose, using a constant $A_m = 10^{-7}$ ($cm^3\,s^{-1}$) and a variable $A_D$ ($s^{-1}$) (1): $10^{-2}$, (2): $10^0$, (3): $10^2$, (4): $10^4$, (5): $10^6$.

function of dose in the localized model of this paper.

The TL peaks obtained from the simulation as a function of the dose are shown in Fig. 5, which shows the shift of the $T_m$ as a function of dose for a fixed values of $A_m = 10^{-7}\,cm^3\,s^{-1}$. The simulated curves are for values of $A_D$ (1): $10^{-7}\,s^{-1}$, (2): $10^0\,s^{-1}$, (3): $10^2\,s^{-1}$, (4): $10^4\,s^{-1}$, (5): $10^6\,s^{-1}$. The general behavior is a shift toward lower temperatures as the dose increases; this behavior is very similar to that observed previously in the delocalized OTOR model.

Fig. 6 shows the symmetry factor $\mu_g$ as a function of the dose using the same parameters as in Fig. 5. It is interesting to note that the curves (1) and (2) which correspond to low $A_D$ values correspond to first order kinetics (see these curves in Figs. 2–4). Furthermore, when the value of $A_D$ approaches the value of $s$ (in which case the PDB is satisfied), the $\mu_g$ values tend to 0.52 which corresponds to second order kinetics, using the terminology of delocalized models.

## 5. Analysis of TL peaks using peak shape methods (PSM) and computerized glow curve deconvolution (CGCD)

In this section we will investigate and analyze in detail the simulated TL peaks from the *localized* transition model, by using well-known methods previously developed for *delocalized* models.

In TL peaks derived in a delocalized model, the activation energy $E$ is evaluated using either the peak shape methods (PSM), or using a computerized glow curve deconvolution (CGCD) analysis.

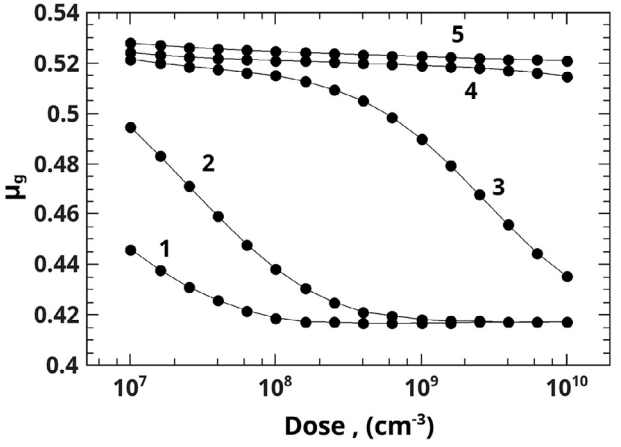


**Fig. 6.** Symmetry factor as a function of dose using $A_m = 10^{-7}$ ($cm^3\,s^{-1}$) and $A_D$ ($s^{-1}$) (1): $10^{-7}$, (2): $10^0$, (3): $10^2$, (4): $10^4$, (5): $10^6$.

### 5.1. Peak shape methods

PSM methods are based on general order kinetics [28–30], and on mixed order kinetics [31]. In this section we apply these well known methods of analysis to the TL peaks generated by the localized model in this paper.

The software used for the simulations can evaluate any geometrical characteristic of the simulated peak, and the mean values of all evaluated $E$ values are listed in Table 1. In all cases the $E$ values from the PSM methods agree with the input $E$ values, with an accuracy better that 1%. Therefore, all geometrical characteristics of TL peaks evaluated in the localized transition model, behave exactly in the same way as the corresponding characteristics of TL peaks evaluated from the delocalized models.

### 5.2. CGCD method

In a similar manner, we apply CGCD methods to the simulated TL peaks, by using the analytical general order kinetic equation [32], and the GOT analytical equation obtained using the Lambert $W$ function [26,33].

In modern software packages, the Lambert function $W(z)$ is a built-in function, similar to any other transcendental function like sine, cosine etc. In the present work the ROOT data Analysis Framework was used [34]. All fittings were performed using the MINUIT program [35] released in ROOT, which is a physics analysis tool for function minimization. The Lambert function $W(z)$ and the exponential integral function $Ei\left[-\frac{E}{kT}\right]$ are implemented in ROOT through the GNU scientific library (GNU GSL)[36].

The results of the curve fittings are also shown in Fig. 7. Using the general order expression for TL, the fit of peaks with $\mu_g$ between 0.42 and 0.52 is excellent. In a similar manner, the fit with the analytical GOT equation using the Lambert function was also very good, giving a Figure of Merit value of FOM = 0.0001. Furthermore, the behavior of $T_m$ and $b$ for the general order fits, and of $T_m$ and $R$ for the GOT

**Table 1**
Output activation energy values in (eV) evaluated using the general order kinetics (GOK) and mixed order kinetics (MOK) peak shape methods (PSM). The reference value is $E = 1.0\,eV$.

| Variable | GOK PSM | MOK PSM |
|---|---|---|
| $A_D$ | $E = 1.006 \pm 0.001$ | $E = 1.014 \pm 0.005$ |
| Dose | $E = 1.01 \pm 0.01$ | $E = 1.01 \pm 0.04$ |
| Curve Fitting | GOK fitting | Lambert $W$ fitting |
| | $E = 1.015 \pm 0.02$ | $E = 0.999 \pm 0.0004$ |

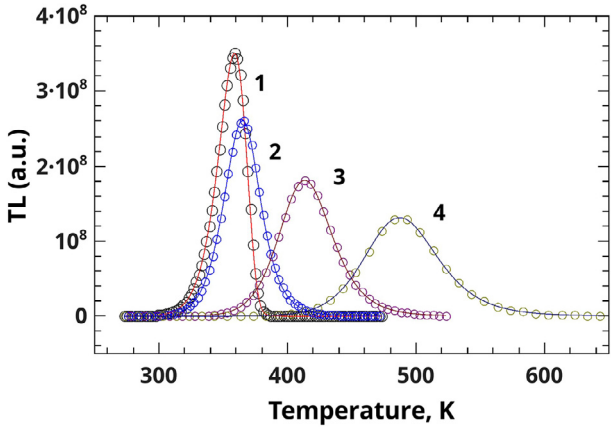


**Fig. 7.** Comparison between peaks derived by numerical solution of differential equation represented by the open circles with numerically evaluated from the analytical solution based on Lambert W function with $A_D$, ($s^{-1}$). (1) $10^{-7}$–$10^{2}$, (2): (3): $10^{5}$ and 4: $10^{7}$.

analytical equations is exactly the same as the one obtained from the PSM method. The results are shown in Figs. 3–6. It is therefore concluded that the PSM and CGCD methods can also be applied to localized TL peaks.

## 6. Testing the analytical expressions for TL and LM-OSL

In the present work we derived analytical expressions given by the master Eq. (15), representing peaks in the localized transition model. It is important to test if these analytical equations give the same results as the solution of the system of differential equations in the model. The procedure followed is:

- A TL peak is generated from the numerical solution of the differential equations.
- The same parameters are used in the analytical expression given by Eq. (15).
- The two peaks are compared with each other.

Examples of this comparison procedure are shown in Fig. 7 for TL peaks, and in Fig. 8 for LM-OSL peaks. In both figures the open circles correspond to the peaks generated by the numerical solution of differential equations, and the solid lines correspond to the peaks evaluated using the master analytical expression given by Eq. (15), along with Eq. (17) for TL and Eq. (18) for LM-OSL. In all cases the agreement between numerically derived and analytically evaluated peaks is at the sixth significant figure. This means that the master equation Eq. (15) is an analytical expression which can describe accurately any stimulated luminescence experiment within the localized transition model studied in this paper.

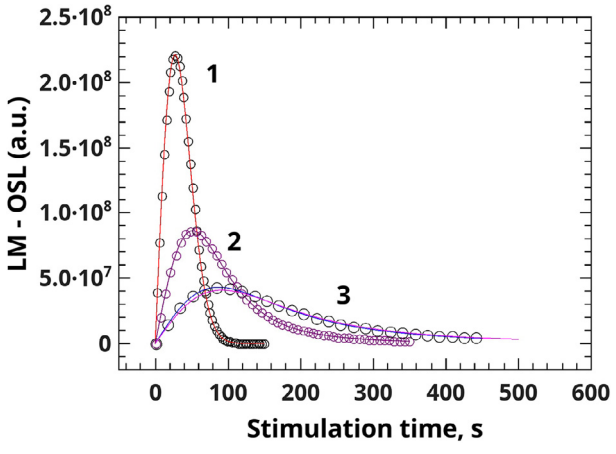


**Fig. 8.** Comparison of LM-OSL peaks derived by numerical solution of differential equations (open circles), with the analytical solution based on Lambert W function (solid lines). (1) $\lambda = 0.2\ s^{-1}$ and $A_D = 10^{-7}$–$10^{0}\ s^{-1}$, (2): $\lambda = 2\ s^{-1}$ and $A_D = 10^{3}\ s^{-1}$ (3): $\lambda = 4\ s^{-1}$ and $A_D = 10^{5}\ s^{-1}$.

## 7. Discussion

### 7.1. The numerical results of Bull [4]

In this section we discuss the numerical results of Bull [4], since these are the standard example of presenting the localized model in luminescence textbooks [1,2,8]. Bull [4] assumed applicability of the PDB (i.e. $A_D = s$), and also assumed that only the nearest neighbor recombination should be considered because the probability of recombination with holes farther away is significantly smaller. This is a rather strict set of assumptions for several reasons. The first reason is in cases of very high local electron and hole densities, electrons can interact with several of their neighbors and are not restricted to their nearest neighbor interactions (Pagonis and Truong [18]). The second reason is that a single value of $\gamma = A_m$ m corresponds to a specific irradiation dose, since the value of $m$ depends on the irradiation conditions. The third reason is that three differential equations with three variables become three differential equations with two variables; as a result of this simplification, the solution of the system of differential equations follows first order kinetics. It is noted, however, that the occurrence of first-order kinetics is not directly related with the principle of detailed balance (PDB), since the equations given by Chen and Kirsh [1] result in a first-order equation without the PDB assumption.

Fig. 9 shows the TL peaks simulated using the model and parameters of Bull [4], in which the PDB is assumed to hold, and the recombination rate is given by $A_m m = \gamma =$ constant. It is noted that all the peaks (4)–(8) in Fig. 9 obey the PDB and have peak maxima in the range 500–2000 K, while theactivation energy is only $E = 0.8$ eV. These results are in opposition to all experimental work, since no TL peaks have been reported in this high temperature range with such a low activation energy. It is simply very difficult to conceive that a temperature of 2000 K is needed to empty thermally a trap with $E = 0.8$ eV. The unlikely physical explanation in this case would be that the electron will be excited and trapped billions of times before recombining.

### 7.2. Further comments on the PDB

The localized model studied here describes not only TL, but also

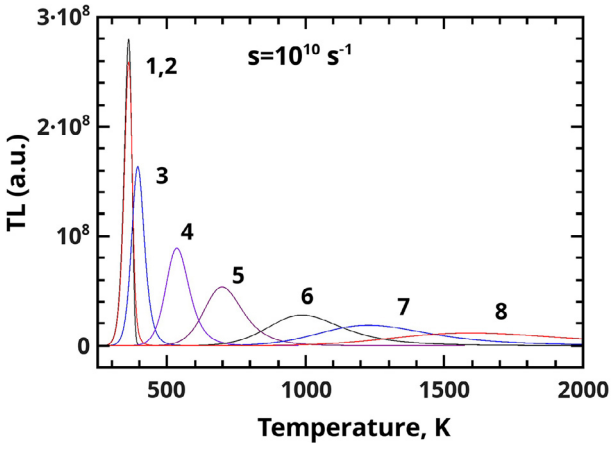


**Fig. 9.** TL peak sequence from the parameters and model by Bull [4], with $n_0 = 10^{10}\ cm^{-3}$ and variable $A_m$ ($cm^3\ s^{-1}$) (1): , (2): $10^{0}$, (3): $10^{-1}$, (4): $10^{-4}$, (5): $10^{-6}$, (6): $10^{-8,}$ (7): $10^{-9}$, (8): $10^{-10}$.

LM-OSL, CW-OSL, ITL etc. The fulfillment of PDB in TL requires the de-excitation coefficient $A_D$ to be equal to the frequency factor $s$. This raises the question, does the PDB apply to these other phenomena?.

Let us consider the case of continuous wave infrared stimulated luminescence (CW-IRSL) in feldspars, which is described by a localized model similar to the one in this paper. The rate of optical excitation in these types of experiments is known to be of the order of $\lambda = 1-5\ s^{-1}$. If we apply the PDB in such a system, then the de-excitation rate would be $A_D = \lambda = 1-5\ s^{-1}$, corresponding to a luminescence lifetime of $\tau = 1/\lambda = 0.2-1$ s.

However, such a very long value of the luminescence lifetime would contradict time-resolved experiments. In general, the luminescence lifetime depends on the material and on the types of experiment involved. Time-resolved measurements in quartz reveal that the lifetime of electrons in the conduction band are in the region of milliseconds, while internal transitions within the recombination center may have luminescence lifetimes of the order of tens of microseconds [37]. On the other hand, the measured lifetimes from time-resolved CW-IRSL experiments in feldspars are in the region of microseconds up to a few millisecond [38,39],while Clark et al. [40] measured lifetimes of the order of nanoseconds.

Considering these experimental results, serious doubts are justified about the applicability and validity of the PDB in TL, and in other stimulated luminescence phenomena.

## 8. Conclusions

This work presented a re-appraisal of localized model in the literature, by lifting two previous restrictions in the model. First it is assumed that the PDB does not apply in systems which are not in thermal equilibrium, and the consequences were examined by extensive simulations. In addition, it is assumed that electrons may interact with many of their neighboring holes, so that the recombination rate depends on both the concentrations of electrons and holes.

The conclusions from this study can be summarized as follows:

- The localized transition model can generate a great variety of single peaks. The decisive parameter in the model is the de-excitation constant $A_D$ , which was varied in the broad region of 10 orders of magnitude.
- All TL peaks generated by the localized transition model were described very well by the peak shape methods, and the analytical TL expressions for the GOK and GOT expressions previously derived for delocalized models.
- All peaks evaluated with the localized transition model have very similar characteristics with the peaks evaluated using a delocalized model.
- In the present work the differential equations describing the localized transition model were analytically solved using the Lambert W function.
- The analytical solutions gave new analytical expressions for TL, LM-OSL, CW-OSL and ITL experiments.

## References

[1] R. Chen, Y. Kirsh, Analysis of Thermally Stimulated Processes, Pergamon Press, 1981.
[2] R. Chen, S.W.S. McKeever, Theory of Thermoluminescence and Related Phenomena, World Scientific, 1997.
[3] A. Halperin, A.A. Braner, Phys. Rev. 117 (1960) 408.
[4] R.K. Bull, J. Phys. D: Appl. Phys. 42 (1989) 1375.
[5] R. Templer, Radiat. Prot. Dosim. 17 (1987) 493.
[6] A.J. Mandowski, J. Phys. D: Appl. Phys. 38 (2005) 17.
[7] V. Pagonis, J. Phys. D: Appl. Phys. 38 (2005) 2179.
[8] R. Chen, V. Pagonis, Thermally and Optically Stimulated Luminescence: A Simulation Approach, Wiley, 2011.
[9] M. Kumar, G. Chourasiya, R.K. Kher, B.C. Bhatt, C.M. Sunta, Indian J. Phys. 85 (2011) 527.
[10] Y.S. Horowitz, I. Eliyahu, L. Oster, Radiat. Prot. Dosim. (2015) 1–17.
[11] V. Pagonis, R. Chen, Ch. Kulp, G. Kitis, Radiat. Meas. 106 (2017) 3.
[12] M. Jain, B. Guralnik, M.T. Andersen, J. Phys. Condens. Matter 24 (2012) 385.
[13] G. Kitis, V. Pagonis, J. Lumin. 137 (2013) 109.
[14] G. Kitis, G.S. Polymeris, I.K. Sfampa, M. Prokic, N. Meriç, V. Pagonis, Radiat. Meas. 84 (2016) 15.
[15] I.K. Sfampa, G.S. Polymeris, V. Pagonis, E. Theodosoglou, N.C. Tsirliganis, G. Kitis, Nucl. Instr. Meth. Phys. Res. B 359 (2015) 89.
[16] I.K. Sfampa, G.S. Polymeris, N.C. Tsirliganis, V. Pagonis, G. Kitis, Nucl. Instr. Meth. Phys. Res. B 320 (2014) 57.
[17] G.S. Polymeris, V. Pagonis, G. Kitis, Radiat. Meas. 97 (2017) 20.
[18] V. Pagonis, P. Truong, Phys. B 531 (2018) 171.
[19] J.L. Lawless, R. Chen, D. Lo, V. Pagonis, J. Phys.: Condens. Matter. 17 (2005) 737.
[20] A.M. Sadek, G. Kitis, J. Lumin. 183 (2017) 533.
[21] P. Kelly, J. Laubitz, P. Braunlich, Phys. Rev. B 4 (1971) 1960.
[22] A. Opanowicz, Phys. Status Solidi, A 130 (1992) 207.
[23] J.P. Lloyd, G.E. Pake, Phys. Rev. 94 (3) (1954) 579.
[24] M.J. Klein, Phys. Rev. 97 (6) (1954) 1446.
[25] J. Thomsen, Phys. Rev. 91 (5) (1953) 1263.
[26] G. Kitis, N. Vlachos, Radiat. Meas. 48 (2012) 47.
[27] R.M. Corless, G.H. Gonnet, D.G.E. Hare, D.J. Jeffrey, D.E. Knuth, Adv. Comput. Math. 5 (1996) 329.
[28] R. Chen, J. Appl. Phys. 40 (1969) 570.
[29] R. Chen, J. Electrochem. Soc. 116 (1970) 1254.
[30] G. Kitis, V. Pagonis, Nucl. Instrum. Methods Phys. Res. B 262 (2007) 313.
[31] G. Kitis, R. Chen, V. Pagonis, Phys. Stat. Sol. (a) 205 (2008) 1181, https://doi.org/10.1002/pssa.200723470.
[32] G. Kitis, J. Gomez Ros, J.W.N. Tuyn, J. Phys. D: Appl. Phys. 31 (1998) 2636.
[33] A.M. Sadek, H.M. Eissa, A.M. Basha, G. Kitis, J. Lumin. 146 (2014) 418.
[34] ROOT, A data Analysis Framework, https://root.cern.ch.
[35] MINUIT, A physics analysis tool for function minimization. Released in ROOT.
[36] GSL-GNU Scientific Library, www.gnu.org/software/gsl.
[37] M.L. Chithambo, C. Ankjrgaard, V. Pagonis, Phys. B 481 (2016) 8.
[38] C. Ankjrgaard, M. Jain, J. Phys. D: Appl. Phys. 43 (2010) 255502.
[39] M. Jain, C. Ankjrgaard, Radiat. Meas. 46 (2011) 292.
[40] R.J. Clark, I.K. Bailiff, M.J. Tooley, Radiat. Meas. 27 (1997) 211.